Proceedings of the National Conference on Cryogenics for Space (NCCS-2019)
December 12-14, 2019, LPSC, Thiruvananthapuram, India.

NCCS-2019-1014

Challenges in designing a POGO suppression device for Cryo environment

Sunny Mitra*, Mathew Saxon A., Aneesh Rajan, Sajeev P.

Earth Storable Engines and Stages Entity, Liquid Propulsion Systems Centre, ISRO, Thiruvananthapuram
*Corresponding Author: sunnymitra111@gmail.com

ABSTRACT

The pogo phenomenon occurs, when the interaction between the longitudinal modes of vibration of the vehicle structure and the liquid propulsion system becomes unstable. To avoid this harmful effect a pogo suppression device is installed in feedlines which helps to decouple these two frequencies. Generally accumulator type of pogo corrector is used in launch vehicles. But for cryogenic feedlines, providing pressurization with a gas is difficult, hence a different design with bellow spring configuration is used to design the pogo corrector for the LOX feedline of semi-cryogenic stage being developed. It has some inherent advantages of no specific orientation requirement and low dead weight.

This paper illustrates the challenges in designing a pogo corrector for cryo environment. Firstly the procedure of decoupling the structural and feedline frequencies is explained. The iterative procedure of finding the optimized design considering minimum size and weight of the system is discussed in detail. Other options with a spring material suitable for cryogenic environment and also with better properties than SS302 has also been looked into. For higher pressure applications further modifications are also considered such as nesting of springs or internal pressurization of the pogo corrector with a non-reactive gas. Finally the selected bellow and spring parameters is presented in this paper

Keywords: Pogo corrector, Pogo suppression device

NOMENCLATURE

K	-Total Stiffness.
Ks	-Spring stiffness.
Kb	-Bellow stiffness.
Ab	-Bellow effective area.
ρ	-Propellant density.
Ca	-Compliance required.
Nb	-Number of bellow convolutions.
δn	-Allowable Axial deformation per convolution
Cδ	-Stiffness per convolution.
Pm	- Mean pressure.

INTRODUCTION

Satellite launch vehicles, which employ liquid stages, are likely to experience pogo instability. This phenomenon occurs, when the interaction between the longitudinal modes of vibration of the vehicle structure and the liquid propulsion system becomes unstable. The propulsion system dynamics is mainly governed by feedlines, pumps and other fluid compliant elements such as bellows etc. When the pogo phenomenon occurs in a liquid rocket, fluctuations are seen in the pump inlet pressure, pump delivery pressure, engine chamber pressure, propellant flow rates, vibration measurements and vehicle acceleration. The pogo phenomenon is usually avoided by incorporating a pogo suppression device at the end of feedline, close to the pump inlet, which modifies the dynamics of the propellant feed system. The preliminary design of the pogo suppression device (PSD) in cryogenic feedline is detailed in this report.

PROBLEM DEFINITION:

Structural dynamic characterization of launch vehicle shows the first axial mode structural frequency. Thus the primary objective of the pogo corrector used in stage is to bring down the propulsion frequency at least below the minimum value of the structural frequency during operation so as to decouple structural and feedline frequencies. Tab. 1 shows the major parameters used as inputs for preliminary design of PSD.

Table 1: Input parameters

Parameter		Unit	Symbol
Feedline configuration	Feedline length from tank bottom to pump inlet	mm	ls
	Feedline diameter	mm	D
	Feedline thickness	mm	t
	Maximum expected pressure in feedline	bar	MEOP

Property of feedline material	Elastic modulus of AA2219 (Stage side)	GPa	Es
	Elastic modulus of SS (Engine side)	GPa	Ee
Properties of propellant	Isentropic Bulk modulus	MPa	B
	Density at feedline temperature	Kg/m3	ρ
Pump related parameters	Pump inlet pressure variation	bar	Pmin-Pmax
	NPSH required	m	NPSHr
	NPSH available	m	NPSHa
	Pump inlet Area	mm2	A1

ESTIMATION OF FEEDLINE FREQUENCY WITHOUT POGO CORRECTOR

The preliminary propulsion system frequency for feed system without PSD is estimated by solving the following transcendental equation (equation 1) [1].

$$2\pi f\left(\frac{l_s}{a_s}\right)\tan\left(2\pi f\,\frac{l_s}{a_s}\right)=\frac{C_s}{C_p} \quad (1)$$

f = Propulsion system frequency, Hz

l_s =Length of feedline from tank outlet to pump inlet, m

a_s = Feedline acoustic velocity, m/s

C_s = Feedline compliance, ms^2

C_p = Pump compliance, ms^2

a) The acoustic velocity in the feedline is dependent on the fluid density ρ and fluid bulk modulus β, as well as, the radial elasticity of feedline given by (E^*t_s/d_s). This parameter is estimated from the following relations.

a_s= sqrt (β_{eq} /ρ) (2)

$\beta_{eq}= \beta / [1+ (\beta^*d_s/E^*t_s)]$ (3)

b) The compliance of the total feedline is the mass change that can be achieved for a unit change in pressure. This is estimated using the equation 4.

$C_s= A_s^*l_s/ (a_s\text{^}2)$ (4)

Where, 'A_s' is the cross sectional area of feedline.

The effective acoustic velocity is computed as,

a_s= sqrt ($A_s^*l_s$ /C_s) (5)

c) Without pogo corrector, the compliance at the pump inlet is due to the pump cavitation compliance only. The cavitation compliance depends on the NPSP at pump inlet. The pump inlet compliance for the booster pumps are only considered for the pogo studies. The pump inlet compliance is to be estimated from pump tests. Due to the lack of test data, for the preliminary design, the empirical correlation developed by S. Rubin [2] using various pump tests data is made use for the pump inlet compliance estimation.

$$\frac{C_p}{A_1}\times 10^5 = -22.4 + 286\left(\frac{S}{S^*}\right) - 274\left(\frac{S}{S^*}\right)^2 + 92.6\left(\frac{S}{S^*}\right)^3 \quad (6)$$

The suction specific speed ratio is the ratio of suction specific speed to the suction specific speed at the cavitation breakdown point (S/S*).

S/S* = (H^*_s / H_s)^(3/4) (7)

where H_s is the suction head & '*'denotes cavitation Breakdown point.

For the present analysis, dispersion band of ±75% is considered on the estimated pump inlet compliance.

The feedline propulsion frequency is computed considering ± 75% dispersion on pump inlet compliance and ± 10% dispersion on feedline compliance. The solution of the transcendental equation (eq.1) is shown in figure 1 and values of propulsion frequencies in Hz considering these dispersions in the data are tabulated in table 2.

Table 2: Estimated frequencies without pogo corrector

C_s \ C_p	(nominal)	(– 75%)	(+ 75%)
(nominal)	9.80	16.71	7.61
(-10%)	9.36	16.16	7.24
(+10%)	10.22	17.20	7.95

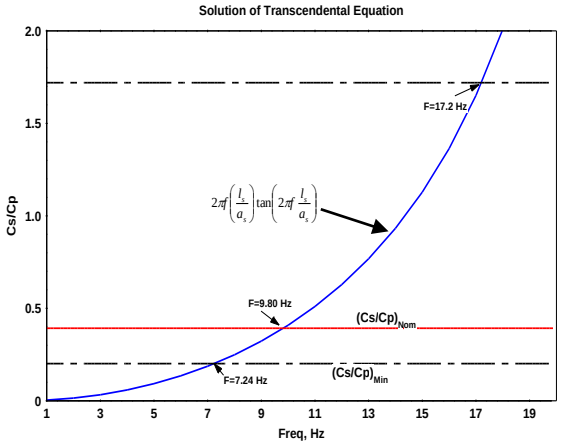

Figure 1: Solution of Transcendental Equation

The estimated propulsion frequencies without pogo corrector are found to be close to structural axial mode frequencies which demands the need of pogo suppression device.

SYSTEM SELECTION AND DESCRIPTION

The selected type has a bellow and spring combination mounted inside, which provides the compliance required to isolate pressure fluctuations (refer figure 2). The accumulator is mounted by flanges to the feedline at the upstream of the pump. This accumulator has operational simplicity, can be mounted in any direction and has no liquid gas interface.

Bellow-Spring type PSD configuration similar to one used due to the following advantages.

a) Standalone - No additional GHe support module required.
b) Low weight (10:1) when compared to gas filled type.
c) No orientation issues.
d) Higher reliability.
The disadvantage is that it offers less flexibility for changing operating parameters.

Bellow-Spring type configuration is best suited if the pump inlet pressure variations are small. The expected pump inlet pressure variation in present scenario is lesser than 2 bar.

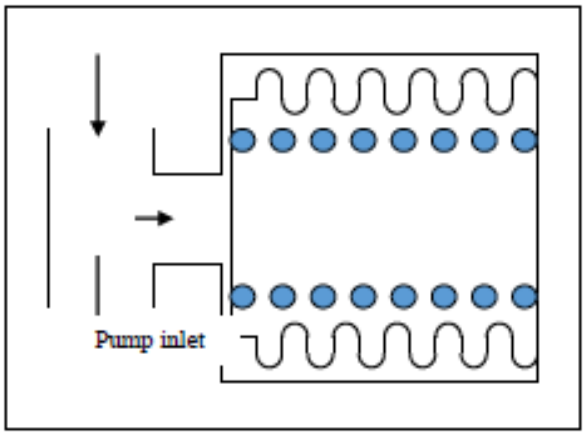

Figure 2: Bellow-Spring Type PSD

The configuration of the proposed bellow-spring type of pogo corrector is given in figure 2. The housing of the pogo corrector encloses a bellow-spring assembly. One end of the bellow is fixed to the housing. The front end of the bellow is closed by an endplate and is free to move. The bellow houses the spring and the stiffness of the bellow and spring together decides the pogo corrector compliance. A guide is provided for the spring, which also acts as a stopper for the end plate. A spacer is used inside the guide for provision to adjust the assembly length of the spring. The inlet passage dimensions and the weight of the moving mass decide the inertance of the pogo corrector.

POGO CORRECTOR DESIGN

A frequency of 7 ± 1 Hz is targeted to achieve frequency separation from structural frequency. The required PSD compliance for a targeted frequency of 7 ± 1 Hz is computed using the equation 8.

$$2\pi f\left(\frac{l_s}{a_s}\right)tan\left(2\pi f\frac{l_s}{a_s}\right)=\frac{C_s}{C_p+C_a} \qquad (8)$$

The required PSD compliance C_a is 3.887 x 10^{-6} ms^2

Table 2: Estimated frequencies with pogo corrector of compliance 3.887 x 10-6 ms2

C_s \ C_p	(nominal)	(– 75%)	(+ 75%)
(nominal)	6.46	7.66	5.70
(-10%)	6.15	7.29	5.42
(+10%)	6.76	8.00	5.96

In bellow-spring type PSD, the combined stiffness of bellow and spring provides the required compliance. The total stiffness required by bellow and spring is computed by following equation.

$$k=k_b+k_s=\frac{A_b^2\times\rho}{C_a} \qquad (9)$$

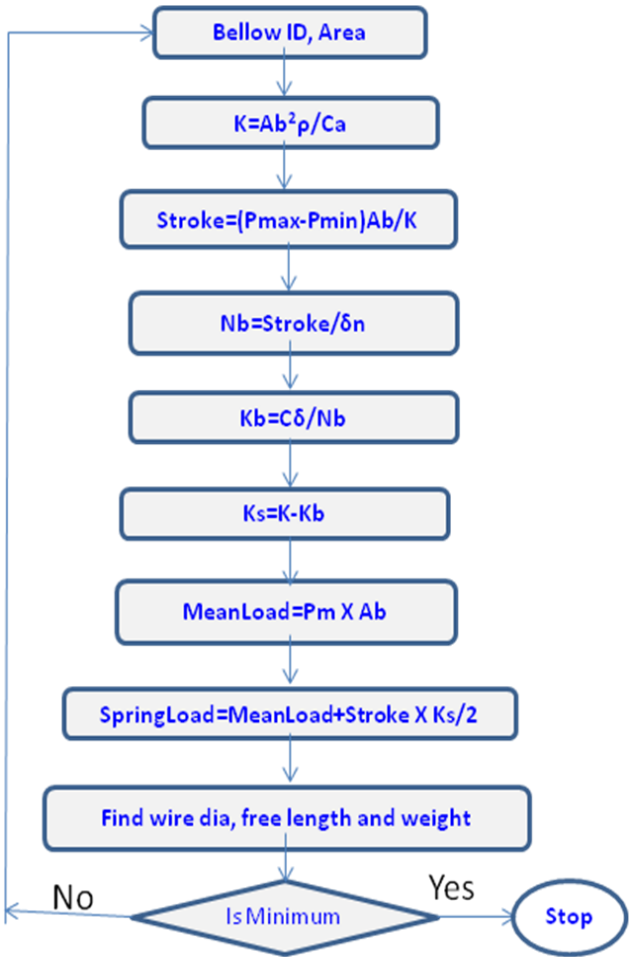

Figure 3: Flow chart for design of PSD

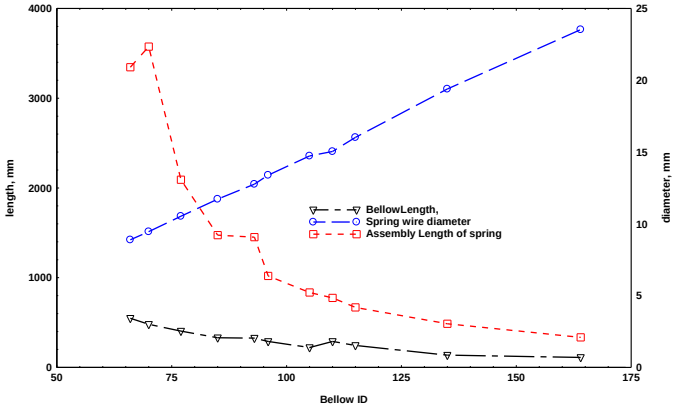

Figure 4: Results of iteration for single spring bellow configuration

For the required compliance, the optimized envelope length of the system with single spring bellow configuration was very high, around 700 mm. Hence a new configuration was thought of with dual spring encapsulated by single bellow. It is one of the preferred designs when the compliance requirement of the PSD is very high.

DUAL SS302 SPRING BELLOW CONFIGURATION

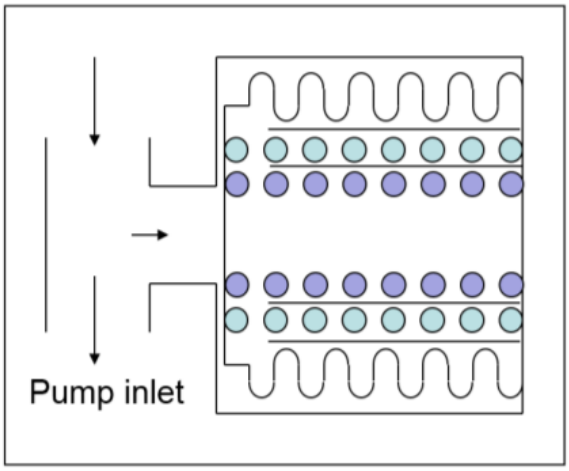

Figure 5: Dual Spring (SS302) Configuration

The configuration is shown in figure 5. It is a parallel spring arrangement so that the spring loads are shared and size is reduced. The combined stiffness of bellow and springs provides the required compliance. The total stiffness required by bellow and springs is computed by following equation.

$$k = k_b + k_{si} + k_{so} = \frac{A_b^2 \times \rho}{C_a} \quad (10)$$

Where ksi and kso are spring stiffness of inner and outer springs respectively. A factor called kf is introduced which is defined as the ratio of stiffness of outer spring to inner spring.

$$k_f = \frac{k_{so}}{k_{si}} \quad (11)$$

Table 3: Procedure of computation of spring and bellow parameters

Parameter	Legend	Formula/ Ref.
Bellow ID, mm	ID_b	Bellow catalogue
Bellow OD, mm	OD_b	Bellow catalogue
Bellow effective area, cm2	Ab	Bellow catalogue
Total stiffness, N/mm	K	$K = \rho \frac{A_b^2}{C_a}$
Stroke, mm	S	$S = \frac{(P_{max} - P_{min})A_b}{K}$
Bellow Deflection, mm	Δ_b	$\Delta_b = \pm\frac{S}{2} \times 1.2$ (Considering a margin of 20%)
Number of bellow Convolutions	N_b	$N_b = \frac{\Delta_b}{\delta_n}$
Bellow stiffness, N/mm	K_b	$K_b = \frac{C_\delta}{N_b}$
Total Spring stiffness, N/mm	K_s	$K_s = K - K_b$
Optimum Spring stiffness ratio	k_f	$k_f = \frac{k_{so}}{k_{si}}$ (found out by iteration)
Outer spring stiffness, N/mm	K_{so}	$K_{so} = \frac{k_f}{1 + k_f} K_s$
Inner spring stiffness , (N/mm)	K_{si}	$K_{si} = K_s - K_{so}$
Mean Pressure, bar	P_m	$P_m = \frac{P_{max} + P_{min}}{2}$
Mean Load, N	F_m	$F_m = P_m \times A_b$
Spring compression at mean position, mm	C_m	$C_m = \frac{F_m}{K_s}$
Design stress of spring, MPa	τ_{design}	www.suhm.net [6]
Mean Load Outer Spring	F_{mo}	$F_{mo} = F_m \frac{k_f}{1 + k_f}$
Spring Load-Outer, N	F_o	$F_o = F_{mo} + \frac{S}{2} K_{so}$
Spring OD-Outer, mm	OD_{so}	$OD_{so} = ID_b - 24$ (Considering a clearance of 24 mm)
Outer Spring wire diameter, mm	d_o	$d_o = \left[\frac{8K_w \times F_o \times D_{so}}{\pi \times \tau_{design}}\right]^{1/3}$
Outer Spring Wahl correction factor	K_{wo}	$K_{wo} = \frac{4C - 1}{4C - 4} + \frac{0.615}{C}$

Mean diameter of outer spring, mm	D_{so}	$D_{so} = OD_{so} - d_o$
Outer Spring Number of active turns	N_o	$N_o = \frac{G{d_o}^4}{8{D_{so}}^3 K_{so}}$
Number of total turns	N_{to}	$N_{to} = N_o + 2$
Initial spring compression, mm	C_i	$C_i = C_m - \frac{S}{2}$
Outer Spring solid length, mm	L_{so}	$L_{so} = N_{to} * d_o$
Outer Spring free length, mm	L_{fo}	$L_{fo} = C_{io} + L_{so} + \frac{S}{0.9}$ (considering 10% margin on stroke)
Outer Spring Pitch	P_o	$P_o = \frac{L_{fo} - 2d_o}{N_{to}}$
Mean Load Inner Spring	F_{mi}	$F_{mi} = F_m - F_{mo}$
Spring Load-Inner, N	F_i	$F_i = F_{mi} + \frac{S}{2} K_{si}$
Spring OD-Inner, mm	OD_{si}	$OD_{si} = OD_{so} - 2d_o - 10$ (with a clearance of 10 mm)
Inner Spring wire diameter, mm	d_i	$d_i = \left[\frac{8K_{wi} \times F_i \times D_{si}}{\pi \times \tau_{design}}\right]^{1/3}$
Inner Spring Wahl correction factor	K_{wi}	$K_{wi} = \frac{4C-1}{4C-4} + \frac{0.615}{C}$
Mean diameter of Inner spring,	D_{si}	$D_{si} = OD_{si} - d_i$
Inner Spring Number of active turns	N_i	$N_i = \frac{G{d_i}^4}{8{D_{si}}^3 K_{si}}$
Inner Spring Number of total turns	N_{ti}	$N_{ti} = N_i + 2$
Inner Spring solid length, mm	L_{si}	$L_{si} = N_{ti} * d_i$
Inner Spring free length, mm	L_{fi}	$L_{fi} = C_i + L_{si} + \frac{S}{0.9}$ (considering a 10% margin on stroke)
Inner Spring Pitch	P_i	$P_i = \frac{L_{fi} - 2d_i}{N_{ti}}$

A computer program in MATLAB is generated to find out the optimum value of this factor kf. The variation of spring assembly length and wire diameter with kf for a specific bellow ID is shown in figure 6. It can be seen that, with the dual spring, the assembly length is reduced. However the assembly length required is still very high. Minimum assembly length required for a bellow ID of 115 mm with dual spring is drastically reduced from the assembly length required for single spring bellow system pogo corrector.

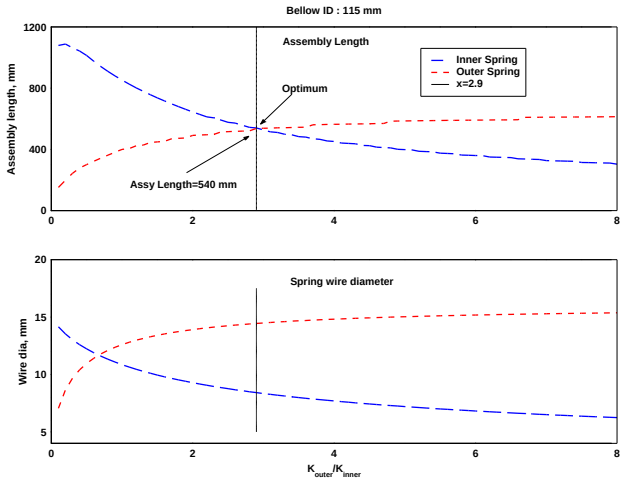

Figure 6: Optimised spring stiffness ratio for a specific bellow ID.

Now for the optimised spring stiffness ratio iterations were done for various bellow sizes.

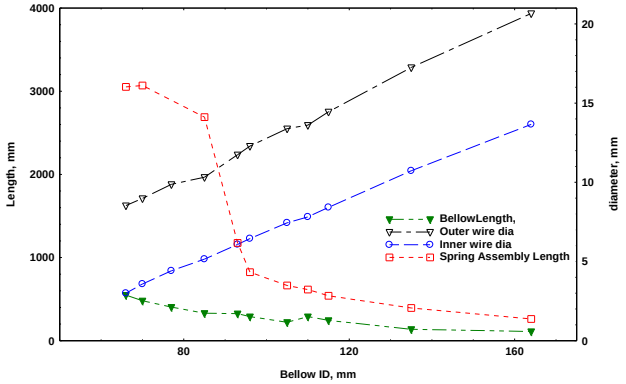

Figure 7: Results of iteration for dual SS302 spring bellow configuration

It is clear from figure 7 that even with dual spring, for SS302 spring material, assembly length is higher than bellow length and resulting envelope is not practical. Hence dual spring configuration in SS302 material is not selected.

CRYO COMPATIBLE HIGH STRENGTH SPRING MATERIAL

A comparison of the tensile strength of various spring materials with wire diameter is shown in figure 8 [4]. It can be seen that Chrome-Silicon gives the highest strength in the entire range of wire diameter. But the compatibility of this material at cryo condition is not established. Considering higher carbon content of 0.59%, the material is not likely to be cryo compatible. Hence Chrome-Silicon material is not selected.

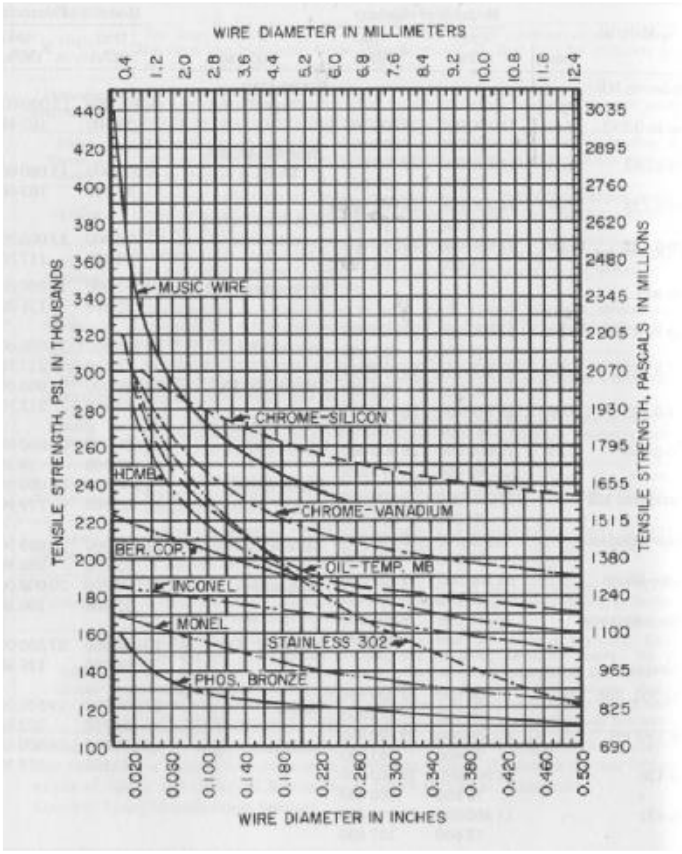

Figure 8: Comparison of tensile strength

Further literature survey on spring materials revealed another material with a trade name MP35N (AMS 5844) [5]. It is a nickel-cobalt alloy with tensile strength of 1793-2086 MPa. It is cryo compatible and can be used up to a temperature of -180^{0}C. The chemical composition of the material as per AMS 5844 is shown in table 3.

Table 3: Chemical composition of MP35N .

Element	min	max
Carbon	--	0.025
Manganese	--	0.15
Silicon	--	0.15
Phosphorus	--	0.015
Sulfur	--	0.010
Chromium	19.00	21.00
Nickel	33.00	37.00
Molybdenum	9.00	10.50
Titanium	--	1.00
Iron	--	1.00
Cobalt	remainder	

Being a new material, the design stress of the material as a function of wire diameter is not available in open literature/standards. The details available from one of spring manufactures web site is shown in table 4 [6].

Table 4: Minimum Tensile strength of MP35N

Physical Properties for SS-MP35N after Drawn and Aged

Sizes	Minimum Tensile Strength, ksi	Minimum Yield, ksi	Minimum Elongation, %	Minimum Reduction of Area, %	HRC
.001 - .005	300	280	1.0	Report	40 - 55
.006 - .100	290	280	4	20	40 - 55
.101 - .170	280	270	4	20	40 - 55
.171 - .250	260	240	5	20	40 - 55
.251 - .437	240	230	6	20	40 - 55
.438 - Over	230	220	8	20	40 - 55

The recommended design stress is taken as 45% of minimum tensile strength [6]. Minimum tensile strength as per table 4 is 230 ksi (1655 MPa).

Design stress, τ_{design} = 0.45x1655=745 MPa

Modulus of rigidity (G) is taken as 80.94 GPa [6].

DUAL MP35N SPRING BELLOW CONFIGURATION

A dual spring configuration with MP35N is proposed as the single spring configuration is found to be bulky. The configuration is same as that shown in figure 5. The same exercises as that was done for dual spring configuration with SS302 is repeated here using properties of MP35N material. Figure 9 shows the results of the iteration for various bellow sizes considering optimum ratio of spring stiffness (k_f).

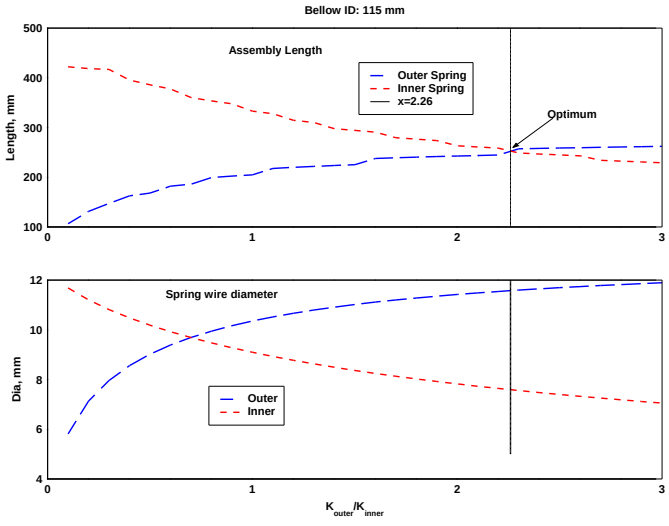

Figure 9: Optimum Ratio of spring stiffness

The optimum value for the ratio of spring stiffness to achieve minimum size for the selected bellow size (115 mm) is 2.26 as shown in figure 9. Since the overall length of the system is ~300 mm, MP35N dual spring configuration can be considered as a possible candidate for pogo corrector of cryogenic feedline.

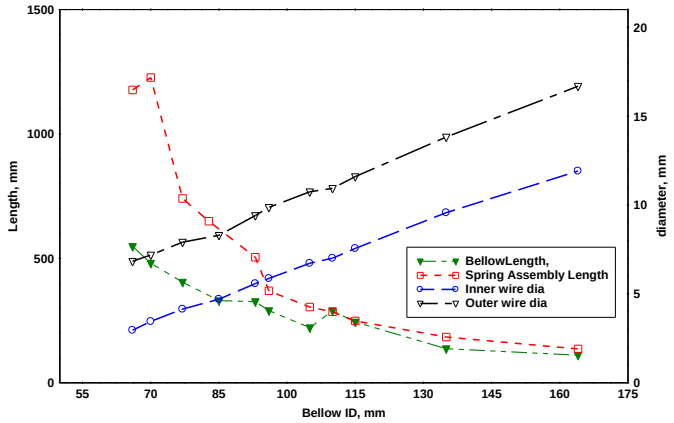

Figure 10: Results of iteration for dual MP35N spring bellow configuration

From figure 10 it is clear that a bellow size of 115mm can give an optimum size of the assembly. Though considerable reduction in length of the assembly can be achieved with higher bellow sizes, it results in increase in diameter of the assembly as well as spring wire diameter. Hence bellow size of 115 mm is selected and detailed computations are carried out.

Table 5: Major PSD Parameters

No	Parameter	Value
1	Bellow Stiffness, N/mm	10
2	Total Spring Stiffness, N/mm	37.44
3	Stiffness of outer spring, N/mm	25.97
4	Stiffness of inner spring, N/mm	11.48
5	Outer Spring free length, mm	372.05
6	Inner Spring free length, mm	384.11
7	Outer Spring wire dia, mm	11.57
8	Inner Spring wire dia, mm	7.59
9	Bellow ID, mm	115
10	Number of Bellow convolutions	33
11	Stroke, mm	53.96
12	Assembly length, mm	310

SINGLE SS302 SPRING WITH GAS FILLED BELLOW CONFIGURATION

It is seen that, the pogo corrector system becomes bulky mainly due to higher pump inlet pressure. The expected variation in pump inlet pressure. For the preliminary design a variation of 2 bar is considered with a margin of ~0.5 bar on either extremes. The load due to the pump inlet pressure directly acts on the end plate which compresses the spring and bellow. The pump inlet pressure load is taken by spring leading to higher spring size in the earlier options. Internal pressurization of the bellow cavity can compensate this higher pump inlet pressure and thereby reduce the overall size. The internal pressure should not exceed the minimum value of pump inlet pressure. Hence an internal pressure of 3 bar is considered in the present study. Helium gas shall be used for pressurisation to avoid any condensation. The overall configuration with internal pressurization is shown in figure 11.

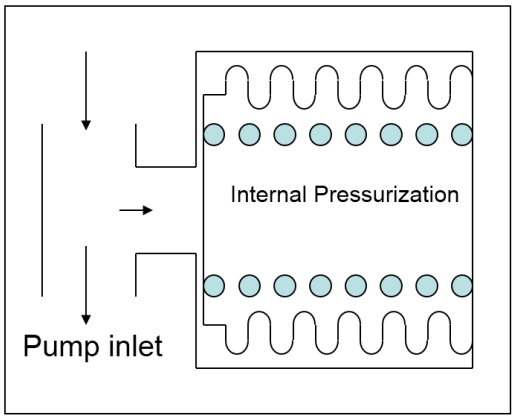

Figure 11: Spring with gas filled bellow configuration

Besides compensating for the pump inlet pressure, the pressurized helium gas inside the bellow cavity acts as a pneumatic spring also. Hence the combined stiffness of bellow, spring and compressed gas (Helium) provides the required compliance. The total stiffness required is computed by following equation.

$$k = k_b + k_g + k_s = \frac{A_b^2 \times \rho}{C_a} \quad (12)$$

Where k_g is stiffness of the pneumatic spring due to pressurized helium gas.

The stiffness of the pneumatic spring can be computed using the following equation.

$$k_g = \frac{\gamma P_g A^2}{V} \quad (13)$$

Where,

K_g = Stiffness of pneumatic spring.

γ = Ratio of specific heat.

P_g = Gas Internal pressure.

A = Cross sectional area.

V = Volume of the gas.

The expected axial deflection of bellow is approximately 33 mm from mean position for the pump inlet pressure variation considered. This deflection of the bellow changes the internal volume and thereby stiffness of the gas also. Hence even if the internal pressure is maintained, gas stiffness is expected to vary with pump inlet pressure. However k_g is considered to be constant in the preliminary design to compute other design parameters. Finally a design check is done with varying gas stiffness.

Bellow size of 115 mm is selected as it was providing an optimum size. The Pogo corrector parameters worked out is shown in table 6.

Table 6: Major PSD Parameters

No	Parameter	Value
1	Spring Material	SS 302
2	Bellow Material	SS 316 Ti
3	Bellow ID, mm	115
4	Total Stiffness, k, N/mm	47.32
5	Bellow Stiffness, k_b, N/mm	10
6	Spring Stiffness, k_s, N/mm	11.36
7	Gas Stiffness, k_g, N/mm	26.08
8	Stroke, mm	53.96
9	Spring wire diameter, mm	9.59
10	Free length of spring, mm	274.26
11	Bellow Length, mm	244.4
12	Assembly length, mm	300

As mentioned above, the gas stiffness is expected to change due to the bellow deflection and consequent volume change. The gas stiffness at both the extreme position of the end plate corresponding to minimum and maximum pump inlet pressure is computed and its effect on pogo corrector is assessed. Table 7 provides the details.

Table 7: Effect of variation of gas stiffness

No	Parameters	P_{min}	P_{max}
1	Bellow length, mm	271.40	217.40
2	Gas Volume, litre	3.47	2.78
3	Gas stiffness, N/mm	23.49	29.32
4	Bellow stiffness, N/mm	10	10
5	Spring stiffness, N/mm	11.36	11.36
6	Total stiffness, N/mm	44.85	50.68
7	Pogo corrector compliance, Ca, ms^2	$4.11x10^{-6}$	$3.636x10^{-6}$

The minimum pogo corrector compliance occurs for the maximum pump inlet pressure condition and it can be seen that the minimum value is 3.636×10^{-6} ms^2. The nominal value of pogo corrector compliance required is 3.887×10^{-6} ms^2. A 10% variation from the nominal value is acceptable and accounted in the pogo analysis. Since the variation is only ~6% for the minimum pogo corrector compliance, the variation in gas stiffness is acceptable. It can be seen that considerable reduction in size is achieved by internal pressurization. The overall length of the system is ~300 mm. The major demerits of this option is the additional requirement of fluid components for internal pressurization.

RESULTS AND DISCUSSION

Since it was found that, a single spring-bellow type configuration is not feasible three design options were studied.

A. Dual spring configuration with SS302 material.
B. Cryo compatible High strength spring material.
C. Internally pressurizing the bellow cavity.

Design Option	Assembly Length, mm	Supporting Fluid components
A	540	Nil
B	310	Nil
C	300	Yes

It is clear that both B and C options seems to be feasible. Considering requirement of supporting fluid components for internal pressurization, option B is more acceptable as it is a standalone configuration.

On a further general note, single SS302 spring with bellow configuration may be used if the assembly length is acceptable. In the current scenario the assembly length was a constraint hence other options were studied. Also if the wire diameter is within acceptable limits, SS302 usage is acceptable. Only if wire diameter of spring is coming very high, there is a need to go to a higher strength cryo compatible material like MP35N, as the wire diameter is inversely proportional to the design strength of the wire material. And gas filled bellows to be restricted for use with higher size bellows as gas stiffness variation is very high in those cases. In dual spring configuration, initial compressions of springs can also be varied as an independent parameter for optimization. In present case it is kept same considering assembling ease.

CONCLUSIONS

Three variants of the spring-bellow pogo suppression device are studied. Dual spring with MP35N is found to be a preferable option for a cryogenic feedline with high pump inlet pressures.

References

[1] A. Rasumoff and R.A. Winje, 'THE POGO PHENOMENON: ITS CAUSES AND CURE', TRW Systems, Houston, Tex., U.S.A.
[2] F.G. Ghahremani and S. Rubin, ‘Empirical Evaluation of Pump Inlet Compliance’, ATR-73 (7257)-1.
[3] Prevention of coupled structure-propulsion instability (POGO) – NASA SP8055.
[4] Spring designers hand book.
[5] www.elgiloy.com.
[6] www.suhm.net